IOP Conf. Series: Materials Science and Engineering **228** (2017) 012007 doi:10.1088/1757-899X/228/1/012007

# Modelling and simulation of a copper slag cleaning process improved by electromagnetic stirring

**H Yang[1], J Wolters[1,*], P Pischke[2], H Soltner[1], S Eckert[3], G Natour[1], J Fröhlich[4]**

[1] Forschungszentrum Jülich, Central Institute for Engineering, Electronics and Analytics, ZEA-1, 52428 Jülich, Germany

[2] RWTH Aachen University, Institute of Heat and Mass Transfer, 52062 Aachen, Germany

[3] Helmholtzzentrum Dresden-Rossendorf (HZDR), Department of Magnetohydrodynamics, 01328 Dresden, Germany

[4] Technical University Dresden (TUD), Institute of Fluid Mechanics, 01062 Dresden, Germany

[*] E-mail: j.wolters@fz-juelich.de

**Abstract**. Electromagnetic stirring in a copper slag cleaning process aims at improving the recovery efficiency of the finely dispersed metallic materials from the waste. In the present study the multiphase problems involved in the slag cleaning process are numerically investigated. An Euler-Lagrange approach with advanced collision and coalescence modelling is employed. The corresponding methodologies are briefly introduced and discussed. Based on the implemented sub-models, the copper recovery is numerically investigated for operating parameters corresponding to industrial pilot plants.

## 1. Introduction

The recovery of valuable metallic material from non-ferrous industrial waste has attracted increasing attention in past decades. In the copper production industry, slags from submerged arc furnaces (SAF) still contain a remarkable amount of copper concentrate [1]. Single SAF furnaces generally produce 700,000 tons of slag per year, which represent a considerable economic recovery potential of the valuable copper material. As a result, a recovery furnace is conventionally arranged to recycle the remaining copper material from the SAF slag, allowing gravitational settling of copper material to the bottom layer due to the density difference (cf. Figure 1). In the slag two thirds of the total copper is present in the form of entrained matte droplets with radii ranging from several micrometers up to millimeters [2], whereas the remainder is dissolved in the slag in the form of copper oxide ($Cu_2O$). A strong direct current (DC) is applied to the slag between the top and the matte layer at the bottom. The electric current generates Joule heat to keep the slag molten and to reduce the level of dissolved copper in the form of $Cu_2O$ through electrode reactions which segregate the dissolved

copper near the anode. The segregated copper aggregates in the form of finely dispersed droplets of 3 to 50 µm diameter [3]. For these small-sized droplets, however, the gravitational settling is too slow for an efficient cleaning process. To increase the separation rate, a magnetic field orthogonal to the electric field is introduced, which generates considerable stirring of the slag. Stirring increases the probability of inter-droplet collisions and coalescence which accelerates the droplet growth and results in a higher settling velocity.

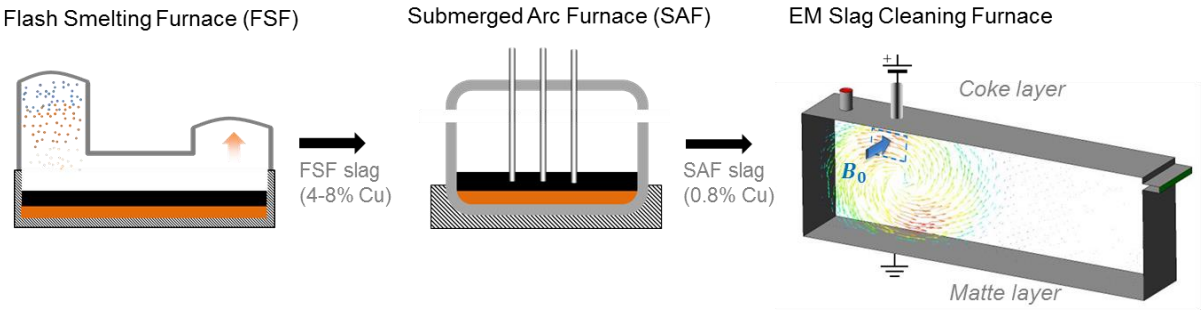


**Figure 1**. Flow diagram of an industrial copper production and slag cleaning process. The novel concept comprises a magnetic field in the recovery furnace to increase the recovery rate by electro-magnetic stirring.

The feasibility of the electromagnetic (EM) copper slag cleaning process was tested at the University of Chile on the laboratory scale [4]. The industrial scale pilot plant was realized by Aurubis AG and SMS group GmbH [5]. The experimental data showed a positive effect of the electromagnetic stirring on the copper recovery, but the relatively low economic efficiency based on the cost of energy have, among other things, so far prevented electromagnetic stirring from being employed commercially. The long-term goal of the present project is to advance the understanding of the complex physico-chemical mechanisms in the copper slag cleaning process and to optimize the industrial process based on CFD calculations. Current numerical work is carried out using the commercial code ANSYS FLUENT.

## 2. Numerical scheme

The numerical investigations of the EM copper slag cleaning process include multiphase modelling, in which the conducting slag is the continuous primary phase and the entrained liquid metal droplets constitute the dispersed secondary phase. The secondary phase features a small volume fraction but a massive number of droplets. Hence, the current simulations are performed with an Euler–Lagrangian scheme, where the primary phase is treated by solving the transport equations on a static grid and the secondary phase is treated as discrete phase in Lagrangian manner.

For the continuous phase, the laminar flow of the conducting slag is driven and stirred by the Lorentz force. The Navier-Stokes equation for an incompressible conducting fluid under the influence of an external electromagnetic field can be expressed as

$$\rho_f \left[\frac{\partial \boldsymbol{U}}{\partial t} + (\boldsymbol{U}\cdot\nabla)\boldsymbol{U}\right] = -\nabla p + \rho_f \boldsymbol{g} + \mu_f \nabla^2 \boldsymbol{U} + \boldsymbol{J_0}\times\boldsymbol{B_0}\,, \tag{1}$$

where $\boldsymbol{U}$ is the flow velocity, $p$ is the pressure, $\boldsymbol{g}$ is the gravity, $\rho_f$ and $\mu_f$ are the density and the viscosity of the slag, respectively. The term $\boldsymbol{J_0}\times\boldsymbol{B_0}$ is the Lorentz force density neglecting the induced fields, which are insignificant in comparison to the superposed fields $\boldsymbol{J_0}$ and $\boldsymbol{B_0}$ in our case.

For the dispersed phase the trajectory of a discrete droplet (or droplet parcel) is computed solving the force balance equation

$$m_d \frac{d\boldsymbol{U_d}}{dt} = \boldsymbol{F_B} + \boldsymbol{F_D} + \boldsymbol{F_E} + \boldsymbol{F_{VM}} + \boldsymbol{F_L} + \boldsymbol{F_{EC}}\,, \tag{2}$$

where $m_d$ and $\boldsymbol{U_d}$ represent the mass and velocity of the droplet, respectively. $\boldsymbol{F_B}$ is the buoyancy force, $\boldsymbol{F_D}$ is the drag force, $\boldsymbol{F_{VM}}$ is the virtual mass force, $\boldsymbol{F_L}$ is the lift force, $\boldsymbol{F_E}$ is the Lorentz force due to the higher conductivity of the droplets, and $\boldsymbol{F_{EC}}$ is the electro-capillary force. Detailed expressions for the individual forces can be found in [4] and [6]. In the stirring zone $\boldsymbol{F_D}$ and $\boldsymbol{F_E}$ are the dominant forces, while in the 'quite zone' the sedimentation of the droplets is dominated by $\boldsymbol{F_B}$ and $\boldsymbol{F_{EC}}$.

## 3. Collision and coalescence of liquid metal droplets in slag

### *3.1. Collision probability*

The growth in droplet size as a result of inter-droplet collisions and coalescence is important in the slag cleaning process. In the present application the direct modelling of collisions for all individual droplets is prohibitive, since their large number would lead to unacceptable computational costs. This problem is avoided by a stochastic model, where the concept of parcels representing a certain number of droplets with the same properties is introduced. The most commonly used algorithm for collision modelling is a purely stochastic Monte Carlo algorithm which is based on the concept of the kinetic gas theory [7] and assumes that the droplets are homogeneously distributed in the collision volume. In this case, the collision probability depends on the mesh resolution, because the collision between droplets of two parcels is only possible when the centers of both parcels are located in the same cell of the grid for the continuous phase. The dependency can become significant for cases with relatively coarse grids as demonstrated by the present authors in [8]. The accuracy could be increased through refining the control volume mesh. However, it may be computationally very costly to introduce such a refinement in geometrically complex simulations and it is difficult to estimate the appropriate mesh-resolution for different cases in advance. To overcome mesh dependency problems of the purely stochastic collision algorithm, a new hybrid Lagrangian collision algorithm was proposed by Pischke et al. [9]. Here, the deterministic algorithm is transferred into a stochastic algorithm by redefining the collision probability assuming a normal distribution of droplets around the centers of the parcels.

To compare both algorithms a test case suggested by Schmidt [10] is considered featuring a cubic domain containing in-homogenously distributed droplets. Here, $10^8$ droplets are assigned to a certain number of parcels, which are exponentially distributed in Y-direction and uniformly distributed in the other two directions. The radii of the droplets vary from 0 µm up to 50 µm and the velocities vary from 0 m/s to 100 m/s. The influence of the grid refinement with a certain number of cells in Y-direction is studied. To obtain statistically relevant results 20 independent runs were performed for each set-up with one time step of 0.1 ms.

Figure 2 shows the root-mean-square error between the average number of collisions predicted by different algorithms and the theoretical number. Compared with the purely stochastic algorithm, the hybrid algorithm is mesh-independent and results in less deviation for the same number of parcels. Due to this advantage, the hybrid algorithm was chosen and implemented for the present simulations.

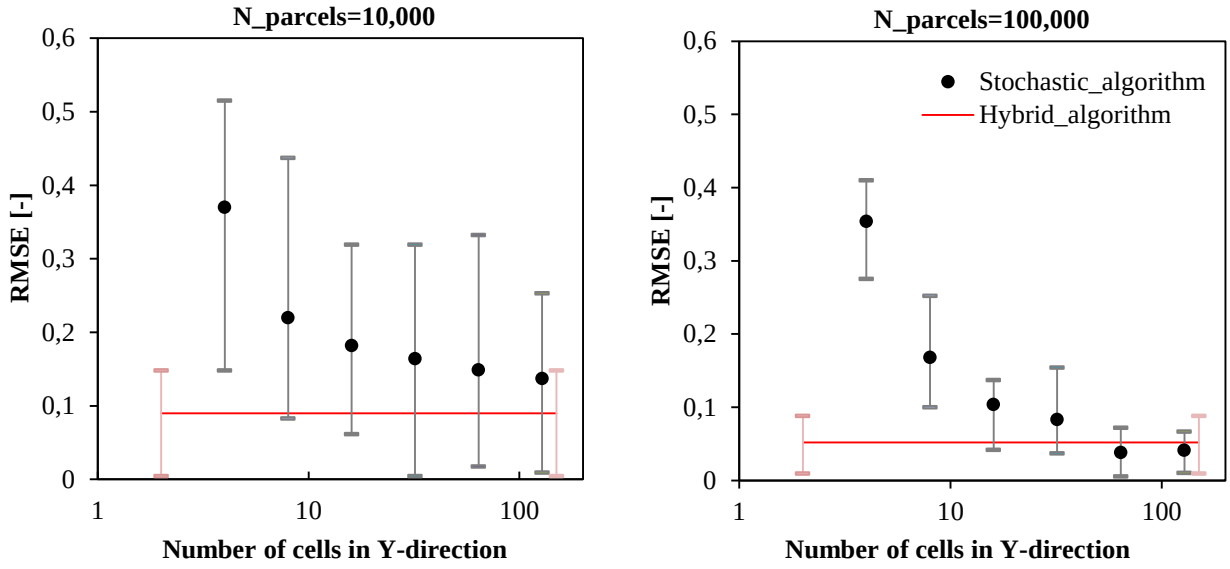


**Figure 2.** Root-mean-square error of the stochastic collision algorithm and the hybrid collision algorithm for an inhomogeneous benchmark case

### *3.2. Collision outcome*

To predict the collision outcome in a stochastic collision modelling, a regime map is required. Generally, it uses two or more parameters to identify the boundary among different possible collision outcomes, here whether coalescence takes place or not. Ready-to-use regime maps, as suggested by Qian and Law [11], are typically established for inertia-driven collisions in a gas-liquid-system with the Weber number (We) as the main criterion. These regime maps, however, are physically not suitable for the present liquid-metal droplet and slag system. First, the collision of droplets in the slag cleaning process features very small Weber numbers ($We \ll 1$), which would always lead to droplet coalescence under the inertia-driven scheme. Second, the regime map has to account for the influence brought by the viscosity ratio between continuous phase and discrete phase. Since experimental results are difficult to obtain in such an opaque, high-temperature environment and consequently no such experimental data could be found by the present authors, the binary collision process between liquid metal droplets was theoretically and numerically studied in more detail to provide a suitable regime map for the collision outcome, taking into account the peculiarities of the slag cleaning process and the physical properties of liquid metal droplets in slags.

Based on our analysis in [12], instead of using a criterion relative to inertia-driven collisions, it was found to be physically more suitable to use the capillary number (Ca) as the main criterion. This includes the influencing factors of shear-driven collisions as encountered in the slag cleaning process. The important dimensionless parameters to characterize the process are

$$\mathrm{Ca} = \mu_f \frac{\dot{\gamma} R}{\sigma}, \quad \mathrm{Re} = \frac{\dot{\gamma} R^2}{\nu}, \quad \psi = \frac{\Delta y}{2R}, \quad \lambda = \frac{\mu_d}{\mu_f}, \quad h'(t) = \frac{h(t)}{R}, \quad t' = \dot{\gamma} t \ .$$

Here, R is the droplet diameter, $\dot{\gamma}$ is the shear rate, σ is surface tension, $\nu$ is the kinetic viscosity, $\mu_d$ and $\mu_f$ are dynamic viscosity for droplet and bulk phase, respectively, h(t) is the film thickness, ψ is the offset ratio of droplets in the direction perpendicular to the relative velocity.

To establish the regime map detailed numerical simulations of individual binary collisions of droplets of equal size were conducted using the volume-of-fluid (VOF) method with high mesh resolution. More details about the setup can be found in [13]. The droplets were positioned in a linear shear flow with a certain offset $\Delta y$ in the direction of the velocity gradient (cf. Figure 3), so that they move on straight lines until they are close enough to interact.

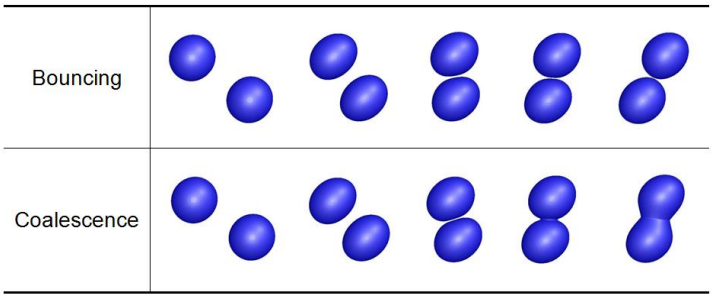


**Figure 3**. Coalescence and bouncing of two colliding droplets in a shear flow simulated with the VOF method.

At this point the confronting interfaces of the two droplets are flattened and the thin film of surrounding fluid starts to drain under the influence of the hydrodynamic forces exerted by the shear flow. Figure 4 exemplarily shows the dimensionless film thickness as a function of time during this process for different capillary numbers and offset ratios.

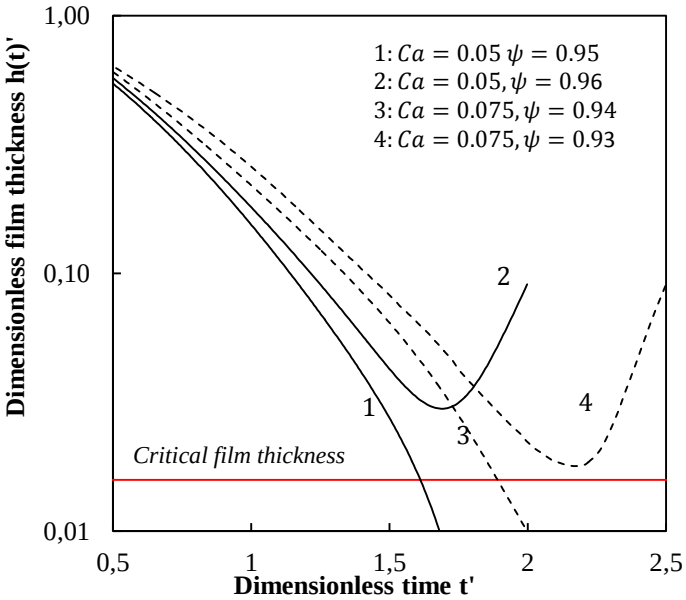


**Figure 4.** Dimensionless film thickness over time in simulations of binary collisions with $\lambda_R = 1$ resulting in coalescence or bouncing, depending on offset ratio $\psi$ and capillary number $Ca$.

The collisions end up in coalescence if the critical value of the film thickness $h_c = \left(\frac{AR}{8\pi\sigma}\right)^{\frac{1}{3}}$ is achieved [14] and the inter-molecular force, becomes comparable with the surface tension force and leads to rupture of the film. Otherwise the droplets will slide along each other's surfaces and the collisions end up in grazed bouncing. A boundary curve separating the regimes of coalescence and bouncing in the plane spanned by the offset ratio and the capillary number can be fitted to the points identified as those with critical offset ratio and is presented in Figure 5 with $\lambda_R = 1$ designating the case of equal particle diameters. In the regime map the scaled capillary number $Ca\left(\frac{R}{\mu m}\right)^{0.84}$ is employed instead of the capillary number $Ca$ itself with the empirical factor deduced from experiments by Hu et al. [15]. It is obvious that for larger droplets the film drainage takes more time than for smaller droplets, if the same capillary number is considered. For unequal-sized collisions an empirical reduction factor of coalescence efficiency $\left(\frac{4\lambda_R}{(1+\lambda_R)^2}\right)^{\kappa}$ in respect of the size ratio $\lambda_R = R_{smaller}/R_{larger}$ suggested by Mousa et al. [16] is employed to extend the regime map. The factor covers the effect that for a constant average radius the coalescence efficiency decreases if the difference in size increases. This decrease in coalescence efficiency is due to the fact that smaller

droplets tend to better follow the curved streamline around the larger droplet in the Stokes regime. The regime map of Figure 5 was used in the simulations reported below.

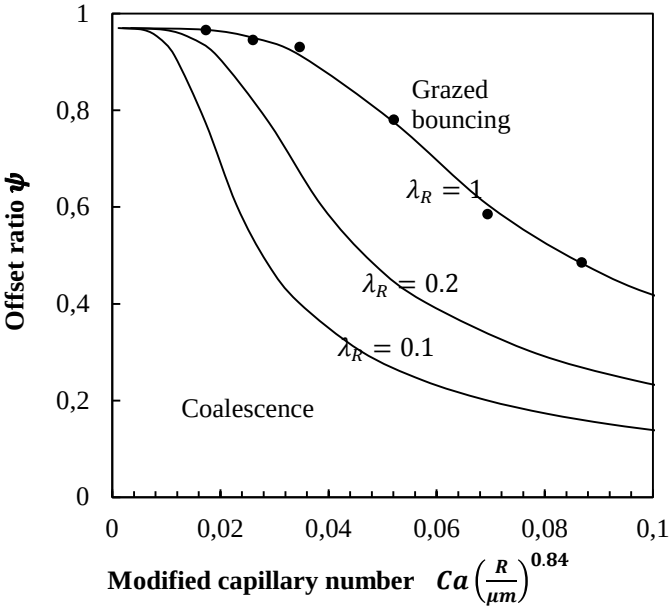


**Figure 5.** Capillary-number-based regime map for the collision result based on VOF simulations with R=0.284 μm.

## 4. Simulation of an industrial pilot plant

Between 2011 and 2012, tests on an industrial scale slag cleaning pilot plant were carried out in Hamburg, Germany. The schematic drawing of the furnace suggested by König et al. [5] is shown in Figure 6. The inner hearth of the furnace has overall dimensions of 2.778 m x 0.578 m x 0.94 m. It is filled with two molten material layers (a 0.14 m high matte layer and a 0.6 m high slag layer) which are covered by a coke layer of 0.2 m thickness. Two graphite electrodes acting as anodes are immersed in the coke layer and contact the slag. Electrode 2 serves only as an emergency electrode and is not considered in the present simulations. The furnace comprises two isolation layers of refractory material. The imposed magnetic field, which is located under the primary electrode, is generated by an electromagnet with a core cross section of 0.3 m x 0.3 m. The important operating parameters are shown in Table 1 and typical material properties are shown in Table 2. Applying the realistic operating parameters and the advanced collision sub-models introduced in the former sections, the preliminary simulations on the practical copper slag cleaning process were carried out. The first results of numerically predicting the copper recovery efficiency for an industrial scale pilot plant will be presented and discussed in this section. The enhanced reduction reaction of dissolved copper content by electromagnetic stirring is also taken into consideration. On the other hand, the heat transfer calculations are not included in the current stage and thus the average temperature of the slag is based on an internal report describing the experiments. Due to the high viscosity of the slag and the low characteristic velocity, the typical Reynolds number at the stirring zone of the investigating case is within the range of $\boldsymbol{O}(1)\sim\boldsymbol{O}(100)$, depending on the strength of the external magnetic fields. Since these values are below 1000, which is the typical boundary value for laminar flows in stirring tanks, the slag flow can be treated as laminar in the calculations.

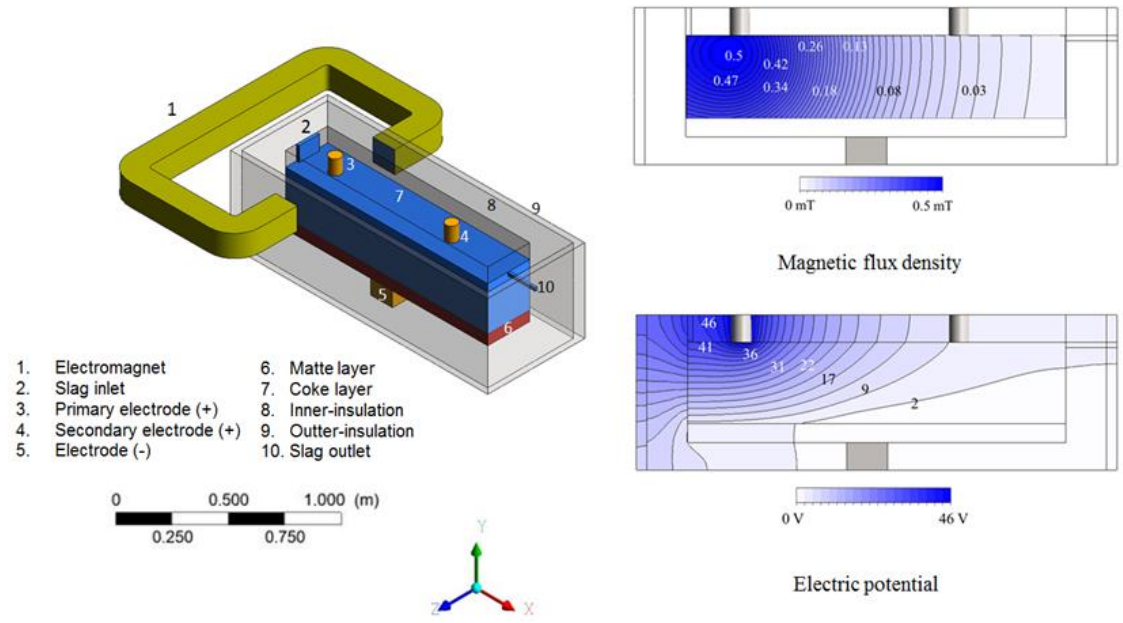


**Figure 6.** Schematic drawing of the slag cleaning furnace in the pilot-plant.

**Table 1:** Important material properties of the copper slag cleaning process.

| | Density ($kg\ m^{-3}$) | Viscosity ($kg\ m^{-1}s^{-1}$) | Electric conductivity ($\Omega^{-1}m^{-1}$) | Resistance of metal/slag interface ($\Omega\ m^2$) |
|---|---|---|---|---|
| Slag | 3600 | 0.1 | 80 | $(0.7 \pm 0.2) \times 10^{-5}$ |
| Matte | 4950 | 0.005 | 5000 | |

**Table 2:** Operating parameters of the slag cleaning furnace in the pilot-plant.

| Slag flow rate (kg/s) | Flow rate matte droplets (kg/s) | Electrode diameter (m) | Total current (kA) | Slag temperature (K) |
|---|---|---|---|---|
| 1.667 | 0.044 | 0.15 | 3 | 1533 |

The injected slag has a copper concentration of 0.8%, of which 2/3 is in the form of matte droplets with the size distribution (50μm to 950 μm) suggested in [2]. The remaining copper is dissolved in the slag as $Cu_2O$, which can be segregated by the following reduction reaction near the coke layer:

$$2(Cu_2O)_{slag} + (C)_{coke} = 4(Cu)_{matte} + CO_2. \quad (3)$$

Here, $(Cu)_{matte}$ will further form the matte inclusion droplets with a diameter assumed uniform and equal to 50 μm. It is also assumed that the matte droplets and the matte generated by reaction have the same composition ($Cu_2S - FeS$). However, it is difficult to evaluate the generation of copper matte based on the reaction rate at an arbitrary time and location, since the concentration of $Cu_2O$ and the slag temperature both keep changing along the reaction interface below the coke layer. An alternative method is to evaluate the change of dissolved copper concentration $\eta(Cu^+)$ at the inlet and outlet. The internal report by SMS group suggests that when the slag is continuously injected

without electromagnetic stirring $\eta(Cu^+)$ can be treated as constant at the inlet $\eta_0(Cu^+) = 0.267\%$ and a 50% reduction can be expected at the outlet. The corresponding mass flow rate of reaction-generated matte $Q_{matte}$ is

$$Q_{matte} = \Delta\eta_0(Cu^+) \cdot \frac{M(Cu_2S)}{M(Cu)} \cdot \frac{1}{0.25} \cdot Q_{slag} \quad , \tag{4}$$

where $M$ represents the molar mass, $Q_{slag}$ is the mass flow rate of slag, and the factor 0.25 reflects the proportion of copper sulphide in the matte inclusions. Due to the massive Joule heat released from the electrode the slag temperature near the primary electrode is much higher than in other parts of the furnace. Hence, it is assumed that the reduction reaction mainly takes place near the coke layer close to the primary electrode.

When the magnetic flux density (B) is applied the stirring velocity of slag is increased and a higher mass transfer coefficient to the reaction interface can be achieved. The change in $\eta(Cu^+)$ with respect to the mass transfer coefficient $k_m$ can be expressed as [17]

$$\Delta\eta(Cu^+) = \eta_0(Cu^+)\left(1 - e^{-t \cdot k_m}\right). \tag{5}$$

The mass transfer coefficient $k_m$ itself can be characterized by the Sherwood number (Sh). The concentration change $\Delta\eta(Cu^+)$ under different magnetic fields can be evaluated by the relationship between the stirring-improved mass transfer coefficient $k_m{}'$ and the mass transfer coefficient without stirring, $k_{m,0}$. When the Schmidt number (Sc) is assumed to be constant, the Ranz-Marshall equation describing the mass transfer can be expressed as [4]

$$\frac{k_m{}'}{k_{m,0}} \sim \frac{Sh'}{Sh_0} \sim \frac{\left(Re^{\frac{1}{2}}Sc^{\frac{1}{3}}\right)'}{\left(Re^{\frac{1}{2}}Sc^{\frac{1}{3}}\right)_0} \sim \left(\frac{U'}{U_0}\right)^{1/2}, \tag{6}$$

where $U'$ is the average velocity of the slag near the coke layer and $U_0$ the slag velocity when no external magnetic field is imposed. The corresponding reaction rates at different magnetic fields can now be estimated by

$$Q'_{matte} = \left(1 - 0.5\sqrt{\frac{U'}{U_0}}\right)\eta_0(Cu^+) \cdot \frac{M(Cu_2S)}{M(Cu)} \cdot \frac{1}{0.25} \cdot Q_{slag} \ , \tag{7}$$

with the corresponding values shown in **Table 3**.

**Table 3:** Generation rate of matte droplets with different magnetic fields.

| Magnetic flux density (mT) | Average velocity near Electrode-1 (m/s) | $\eta(Cu^+)$ at outlet (%) | Generation rate of matte droplets (kg/s) |
|---|---|---|---|
| 0 | 0.00074 | 0.1300 | 0.0111 |
| 5 | 0.01125 | 0.0188 | 0.0206 |
| 20 | 0.02826 | 0.0036 | 0.0219 |

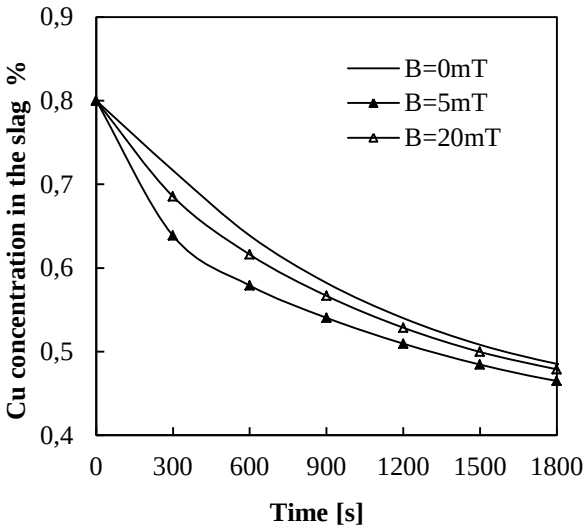


**Figure 7.** Level of copper content over operation time.

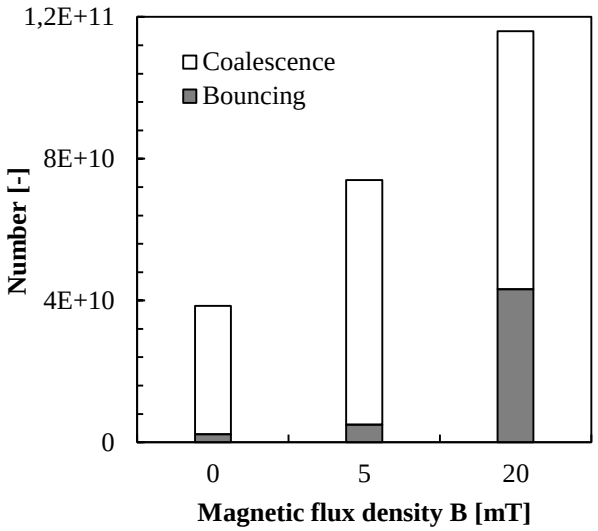


**Figure 8.** Outcomes of the inter-droplet collisions during 0.5 h for different magnetic fields.

The first simulations of the industrial pilot plant were performed with an operating time of t = 0.5 hour. During this time the slag with entrained copper droplets is continuously injected into the furnace while the reaction-generated droplets are simultaneously injected near the primary electrode. The concentration of remaining copper will reach a quasi-constant value after some time of operation beyond the interval covered. During the simulation the overall droplet population ($\sim 10^{10}$) was represented by $\sim 10^{5}$ parcels.

The temporal evolution of the copper content in the slag is shown in Figure 7 for different magnetic flux densities. As expected, compared to the case without electro-magnetic stirring the recovery of matte droplets is increased when introducing the magnetic field. The positive effect, however, decreases beyond certain strength of the magnetic field. This trend was also observed in the experiments. One reason for this is the increased drag force due to the stirred flow which makes settling even of the larger droplets resulting from coalescence more difficult and leads to a higher copper concentration remaining in the slag. On the other hand the increased stirring influences the collision outcome. Although the number of collisions is significantly increased with stronger magnetic fields and corresponding higher relative droplet velocities, the number of collisions resulting in coalescence does not increase any more or even decreases for higher velocities (Figure 8). According to the study in Section 3.2, coalescence as a result of shear-driven collisions is more likely for small impact velocities with similar size of the two droplets involved. As a result, the overall growth in droplets size due to inter-droplet coalescences is not significantly enhanced any more with stronger stirring, at least not enough to compensate the deceleration of sedimentation due to the highly disturbed flow field.

Based on the numerical results, optimization of the device and operating conditions is possible now. First of all the strength of electromagnetic stirring has to be adjusted to maximize the copper recovery rate. Moreover, the currently used C-electromagnet creates a widely spread magnetic field in the furnace causing a large stirring zone - in comparison with the length of the furnace - and compresses the settling zone. The setup of the electromagnet should therefore also be optimized.

A comparison between numerical and experimental results could not be conducted up to now, since some basic parameters and results of the experiments have to be further discussed with SMS group GmbH, such as, for example, the exact size distribution of the matte droplets entrained in industrial slags.

## 5. Conclusions and perspectives

A numerical approach to model an industrially relevant enhancement of a copper slag cleaning process through electromagnetic stirring was developed. An Euler-Lagrangian scheme for solving the multiphase problem was implemented, where slags are defined as continuous phase and liquid-metal droplets are treated as dispersed parcels. For the continuous phase, MHD (magneto-hydrodynamic) calculations on the conducting slag under the influence of orthogonally magnetic and electric fields were performed. For the dispersed phase, tracking of the liquid metal droplet was realized by solving the force balance accounting for the electromagnetic forces.

To predict the growth of the droplet size due to inter-droplet collisions and coalescence, a mesh-independent hybrid Lagrangian collision algorithm was introduced to calculate the collision probability, which has an excellent adaptability in both homogeneous and in-homogeneous cases. Moreover, to correctly predict the collision outcome in the stochastic collision modelling, a new regime map for the collision outcome was developed. It is based on a large number of VOF calculations of the binary collision process taking into account the peculiarities of the slag cleaning process and physical properties of liquid-metal droplets in slags. This regime map is available for use in subsequent now. Moreover, it points to the more general fact that inertia-based regime maps for collisions are not applicable in viscosity-dominated situations and need to be replaced by different ones.

The developed method was then applied to the setup of an industrial pilot plant investigating the efficiency of copper recovery under different imposed magnetic flux densities. Electromagnetic stirring using a relatively weak magnetic field of B = 5 mT significantly increases the generation of copper matte inclusions due to the reduction reaction near the coke layer. Moreover, the increased inter-droplet coalescence rate increases the droplet size and accelerates sedimentation of the droplets. Further enhancement of the magnetic field does not provide considerable improvements in the coalescence efficiency, though, but generates stronger disturbances in the flow field that lead to a decreased sedimentation rate of the droplets. As a result, simply increasing the strength of the imposed magnetic field fails to increase the copper recovery efficiency. Further validation will be performed.

The simulation tool is now ready for optimizing the industrial process, and more detailed calculations of the industrial copper slag cleaning process will be realized in the near future. For example, discontinuous electromagnetic stirring will be considered which seemed promising in the experiments.

## Acknowledgments

The authors acknowledge the financial support from the German Helmholtz Association in the framework of the Helmholtz Alliance LIMTECH, Project A5, and like to thank Mr. König and Mr. Köneke from SMS group GmbH for providing information on the test facilities and for the fruitful discussion on the slag cleaning process.

## References

[1] Schlesinger M and King M 2011 *Extractive metallurgy of copper 5th ed.* (UK: Elsevier)
[2] Warczok A and Riveros G 2003 *Yazawa International Symposium-Metallurgical and materials processing and technology* Volume **2** 417-429
[3] Degel R, Oterdoom H, Kunze J, Warczok A and Riveros G 2008 *Third International Platinum Conference 'Platinum in Transformation'* (Sun City, South Africa) 197-202
[4] Warczok A and Riveros G 2007 *Miner. Eng.* **20** 34-43
[5] König R, Degel R, Rose L, Schmidl J, Kadereit H and Specht A 2013 *TMS Annual Meeting & Exhibition* (San Antonio, USA)
[6] Choo R T C and Toguri J M 1992 *Canadian Metallurgical Quarterly* **31** 113-126
[7] O'Rourke P J 1981 Ph.D thesis Department of Mechanical and Aerospace Engineering Princeton University

[8] Yang H, Wolters J, Pischke P, Soltner H, Eckert S and Fröhlich J 2015 *8th International Conference on Electromagnetic Processing of Materials* (Cannes, France) 255-258
[9] Pischke P, Cordes D and Kneer R 2012 *Int. J. Multiphase Flow* **38** 1–16
[10] Schmidt D 2006 *J. Comput. Phys* **164** 62-80
[11] Qian J and Law C K 1991 *J. Fluid Mech.* **331** 59-80
[12] Yang H, Wolters J, Pischke P, Soltner H, Eckert S and Fröhlich J 2016 *9th International Conference on Multiphase Flow* (Firenze, Italy).
[13] Yang H, Wolters J, Pischke P, Soltner H, Eckert S and Fröhlich J 2017 *12th International Conference on CFD in Oil & Gas, Metallurgical and Process Industries, SINTEF* (Trondheim, Norway)
[14] Chesters A 1991 *Trans. IChemE* **69** 259-270
[15] Hu Y T, Pine D J and Leal L G 1989 *Phys. Fluids* **12** 484-489
[16] Mousa H and van de Ven T G M 1991 *Colloides Surfaces A* **60** 19-38
[17] Reddy R G, Prabhu V L and Mantha R 2003 *High Temp. Mater. Processes* **22** 25-33